UDC 551.511.61 DOI: 10.18698/1812-3368-2022-3-86-95

NUMERICAL INVESTIGATION OF A SUPERSONIC FLOW IN THE NEAR WAKE REGION OF A CYLINDRICAL AFTERBODY

A.M. Molchanov alexmol_2000@mail.ru
D.S. Yanyshev dyanishev@gmail.com
L.V. Bykov bykovlv@mai.ru

Moscow Aviation Institute (National Research University), Moscow, Russian Federation

Abstract

A computational study of a supersonic flow in the base region and the nearest wake of a cylindrical body moving at a supersonic speed have been carried out. A mathematical model of high-enthalpy flows is presented. In this case, the "prehistory" of the flow was taken into account, i.e., the configuration of the computational domain was as close as possible to the real one. The use of various turbulence models for calculating flow in the base region and the nearest wake was analyzed. The following turbulence models were considered: 1) the Spalart — Allmaras model; 2) SST model; 3) standard k–ε model; 4) k–ε model with compressibility correction; 5) k–ε RNG (renormalized group) model; 6) k–ε Realizable model; 7) standard Reynolds Stress (RS) model; 8) RS BSL (Reynolds stress baseline) model. Based on a comparison of the calculation results with experimental data, it is shown that: 1) when calculating the flow in the base region and in the wake of the vehicle, it is very important to take into account the "prehistory" of the flow, i.e., to calculate the flow around the entire vehicle; 2) the best match was obtained using Reynolds Stress models and the k–ε RNG model

Keywords

Computational fluid dynamics, turbulence, external flow, supersonic flow

Received 26.01.2022
Accepted 14.02.2022

Introduction. The theoretical study of a flow in the base area and in the wake of a high-speed vehicle is important in many aerospace applications. The separated flow arising in the base area of such aerodynamic bodies can have a significant effect on various flight characteristics. Low bottom pressure causes drag that affects stability, trajectory and range. The reverse flow can significantly increase the heat flow to the structural elements of the vehicle.

It is generally accepted (see, e.g. [1–3]) that the theoretical approach based on the use of Reynolds-averaged Navier — Stokes equations is not very successful

in describing such flows due to several reasons, such as the instability of the recirculation zone and the difficulty of modeling turbulent characteristics in a compressible mixing layer.

It was shown in [4] that the "prehistory" of a flow has a very large effect on the distribution of parameters in the bottom area and in the wake, i.e., the flow along the cylindrical part of the vehicle and the nose section.

The *purpose of this work* is to analyze the use of various turbulence models for calculating the flow in the base area and in the wake of a high-speed vehicle. And the "prehistory" is taken into account, i.e., the configuration of the computational domain is as close as possible to the real one.

Supersonic, axisymmetric base flow. A schematic diagram of the mean flowfield structure in the near wake of a cylindrical afterbody aligned with a supersonic flow is shown in Fig. 1 [4].

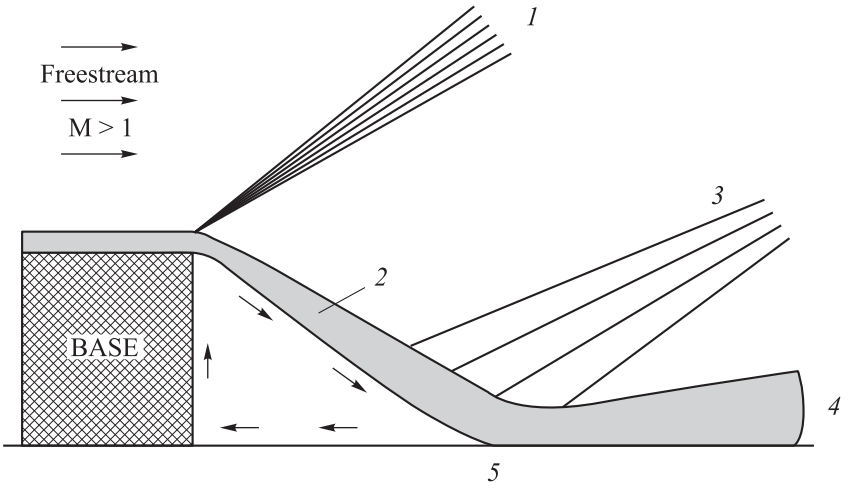

Fig. 1. Flow diagram of base flow in the wake of a vehicle moving at supersonic speed: *1* — expansion waves; *2* — free shear layer; *3* — recompression region; *4* — trailing wake; *5* — rear stagnation point

The supersonic afterbody freestream flow undergoes a strong expansion centered at the base comer as the turbulent boundary layer separates geometrically from the body. A free shear layer is formed which separates the outer inviscid flow from a relatively large recirculation region immediately downstream of the base. The intense turbulent mixing and energy exchange that characterize the free shear layer are important in determining the flowfield properties throughout the near wake including the recirculation region. As the free shear layer approaches the axis of symmetry, a recompression process occurs which eventually realigns the flowfield with the axis. A rear stagnation

point, where the mean velocity vanishes, is located on the centerline and separates the recirculation region from the wake which develops downstream.

Governing equations. To describe the flow of a multicomponent gas mixture, the following system of equations written in vector form is used

$$\frac{\partial \mathbf{U}}{\partial t} + \sum_{i=1}^{3} \frac{\partial}{\partial x^i} \left(\mathbf{F}_C^i - \mathbf{F}_V^i \right) = \mathbf{H},$$

with main vector

$$\mathbf{U} = \begin{pmatrix} \rho \\ \rho u^1 \\ \rho u^2 \\ \rho u^3 \\ \rho E^T \\ \rho C_1 \\ \vdots \\ \rho C_{Nc-1} \\ \rho \mathrm{T}_1 \\ \vdots \\ \rho \mathrm{T}_{Nt} \end{pmatrix},$$

convective vector

$$\mathbf{F}_C^i = \begin{pmatrix} \rho u^i \\ \rho u^i u^1 + \delta^{i1} p \\ \rho u^i u^2 + \ldots + \delta^{i2} p \\ \rho u^i u^3 + \ldots + \delta^{i3} p \\ \rho u^i \left(E^T + p/\rho \right) \\ \rho u^i C_1 \\ \vdots \\ \rho u^i C_{Nc-1} \\ \rho u^i T_1 \\ \vdots \\ \rho u^i T_{Nt} \end{pmatrix},$$

viscous vector

$$\mathbf{F}_V^i = \begin{pmatrix} 0 \\ \tau^{i1} \\ \tau^{i2} \\ \tau^{i3} \\ \sum\limits_{j=1}^{3} u^j \tau^{ij} - q^i \\ -J_1^i \\ \vdots \\ -J_{Nc-1}^i \\ -g_1^i \\ \vdots \\ -g_{Nt}^i \end{pmatrix},$$

source vector

$$\mathbf{H} = \left(0, 0, 0, 0, -\sum_{s=1}^{Nc} h_s^0 \dot{w}_s, \dot{w}_1, \ldots, \dot{w}_{Nc-1}, S_{T,1}, \ldots, S_{T,Nt} \right)^t$$

and Kronecker delta in cartesian frame

$$\delta^{ij} = \begin{pmatrix} 1 & 0 & 0 \\ 0 & 1 & 0 \\ 0 & 0 & 1 \end{pmatrix}.$$

Fluxes are computed using the following formulae:

$$\tau^{11} = \frac{2}{3}\mu\left(2\frac{\partial u^1}{\partial x^1} - \frac{\partial u^2}{\partial x^2} - \frac{\partial u^3}{\partial x^3}\right); \quad \tau^{12} = \tau^{21} = \mu\left(\frac{\partial u^1}{\partial x^2} + \frac{\partial u^2}{\partial x^1}\right),$$

$$\tau^{22} = \frac{2}{3}\mu\left(2\frac{\partial u^2}{\partial x^2} - \frac{\partial u^1}{\partial x^1} - \frac{\partial u^3}{\partial x^3}\right); \quad \tau^{13} = \tau^{31} = \mu\left(\frac{\partial u^1}{\partial x^3} + \frac{\partial u^3}{\partial x^1}\right),$$

$$\tau^{23} = \tau^{32} = \mu\left(\frac{\partial u^2}{\partial x^3} + \frac{\partial u^3}{\partial x^2}\right); \quad \tau^{33} = \frac{2}{3}\mu\left(2\frac{\partial u^3}{\partial x^3} - \frac{\partial u^1}{\partial x^1} - \frac{\partial u^2}{\partial x^2}\right),$$

$$q^i = -\frac{\mu}{\mathrm{Pr}}\frac{\partial h}{\partial x^i}, \quad J_s^i = -\frac{\mu}{\mathrm{Sc}}\frac{\partial C_s}{\partial x^i}.$$

Here ρ is the density of the gas mixture; u^i are velocity components; p is pressure; τ^{ij} is viscous stress tensor; μ is effective coefficient of dynamic viscosity (takes into account both molecular and turbulent transport); C_s is mass fraction of species s; $\dot{w}_s$ is the rate of formation of species s as a result of chemical reactions; N_c is the number of species of the gas mixture; J_s^i is the diffusion flux of the species s; E^T is the thermodynamic part of the total energy; q^i is the density of the heat flux due to thermal conductivity and diffusion; Pr, Sc are the effective Prandtl and Schmidt numbers; h is enthalpy; h_s^0 is the enthalpy of formation of the species s.

The pressure of the gas mixture is the sum of the partial pressures of all species:

$$p = \sum_{s=1}^{N_c} p_s = \sum_{s=1}^{N_c} \rho_s \frac{R_U}{M_s} T = \rho \frac{R_U}{M_\Sigma} T, \tag{8}$$

where T is the temperature; R_U is the universal gas constant; M_s is the molar mass of species s; M_Σ is the apparent molecular weight of the gas mixture,

$$M_\Sigma = \left(\sum_{s=1}^{N_c} \frac{C_s}{M_s} \right)^{-1}. \tag{9}$$

The main system includes parameters characterizing turbulence T_1, $T_2, \ldots,$ T_{Nt}, the choice of which depends on the used turbulence model.

In this paper, the following turbulence models were considered (for the sake of brevity mathematical description of the models is omitted, for their thorough description address, e.g., to [5] and [6]): 1) the Spalart — Allmaras model; 2) SST (shear stress transport) model; 3) standard k–ε model; 4) k–ε model with compressibility correction; 5) k–ε RNG (renormalized group) model; 6) k–ε Realizable model; 7) standard Reynolds Stress (RS) model; 8) RS BSL (Reynolds stress baseline) model.

Results and discussion. The experimental data from [4, 7, 8] was used for testing the calculation method. Free stream parameters: M = 2.5, T = 130 K, p = 30 141 Pa. Body diameter 63.5 mm.

The program *Universe CFD* [9–11], developed at the MAI by the Department of Thermal Engineering, was used for the calculations. We also used the methods and general approaches from [12–14].

The computational grid for flow around the vehicle, the flow in the base region and in the near wake is shown in Fig. 2. It was built as purely structured multiblock grid with quad elements and then converted to unstructured one to use within *Universe CFD* unstructured solver.

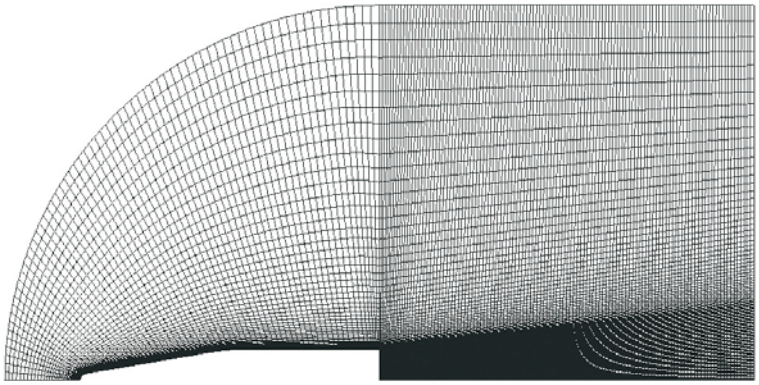

Fig. 2. Computational grid

Grid independence study was performed with different several meshes of different sizes. The one shown on Fig. 2 was found to be optimal to use for all case studies. Its overall size was 16 233 cells.

Figure 3 shows some results of calculating the velocity on axis in the base region and in the near wake using various turbulence models.

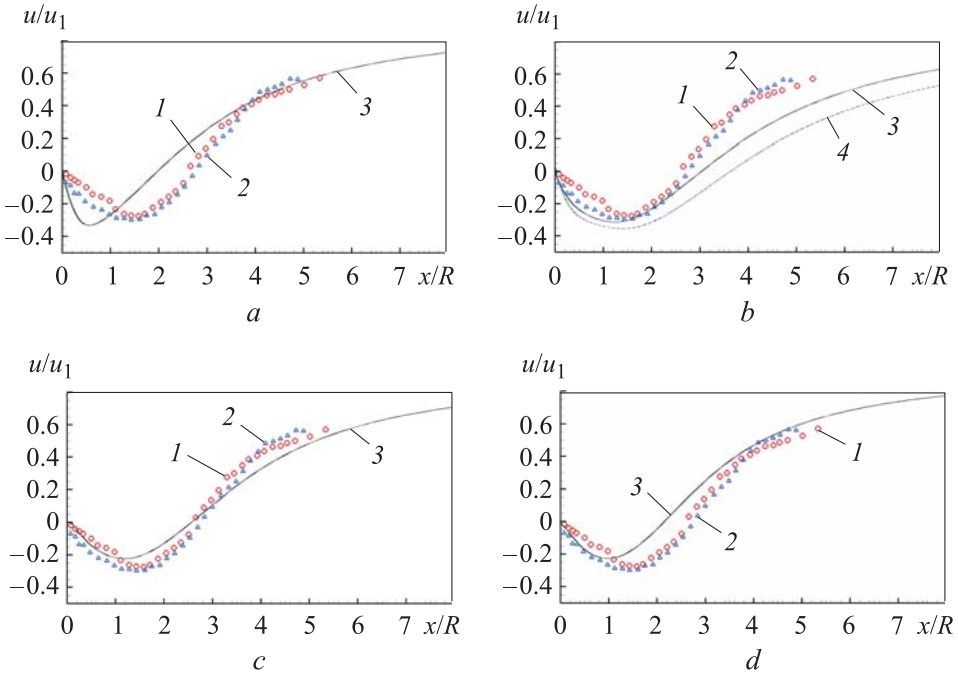

Fig. 3. Axial velocity distribution along centerline in the base region of a cylindrical model in a supersonic flow M = 2.5:

a — the Spalart — Allmaras model; *b* — *k*–ε RNG model; *c* — model RS standard; *d* — model RS BSL; *1* — experiment [3], *2* — experiment [5]; *3*, *4* — calculations (*3* — no compression correction, *4* — with compression correction)

Figure 4 shows the dependence of the base pressure on the freestream Mach number. The standard RS model as well as RS BSL model are quite successful from this point of view.

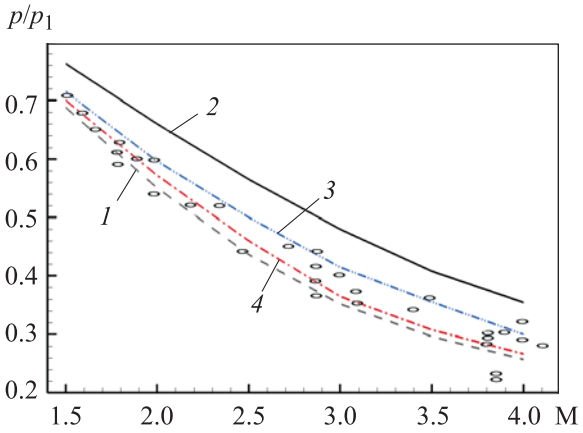

Fig. 4. Base pressure ratio versus freestream Mach number:
circles — experimental data [6]; *1* — SST turbulence model; *2* — *k*–ε RNG turbulence model; *3* — standard RS turbulence model; *4* — RS BSL turbulence model

In this view it is interesting also to look at Reynolds shear stress values obtained via RS BSL model (Fig. 5). As it can be seen from the figure, the obtained profiles of the Reynolds shear closely resemble experimental data.

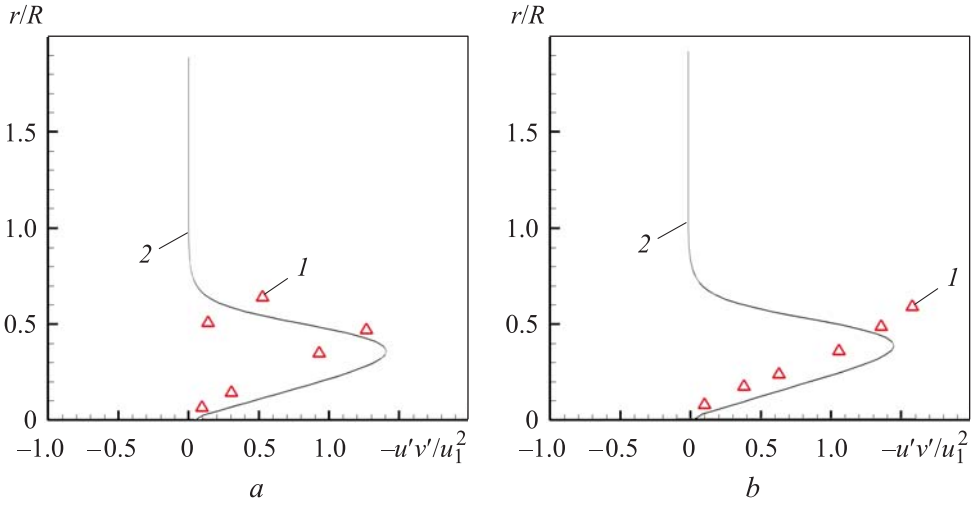

Fig. 5 (beginning). Radial distribution of dimensionless Reynolds shear stress $\left(-\overline{u'v'}/u_1^2\right)$ in different sections:

a — *x*/*D* = 1.26; *b* — *x*/*D* = 1.42; *1* — experimental data as per [8]; *2* — RS BSL turbulence model

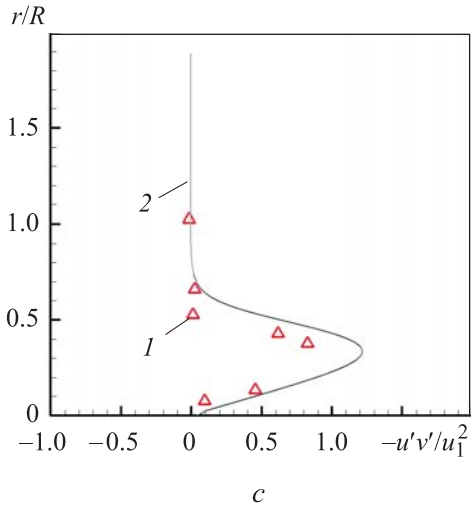

Fig. 5 (end). Radial distribution of dimensionless Reynolds shear stress $\left(-\overline{u'v'}/u_1^2\right)$ in different sections:

c — *x*/*D* =1.73; *1* — experimental data as per [8]; *2* — RS BSL turbulence model

Although, Reynolds stress models take much more computational effort (5 equations are being solved in 2d case and 7 in 3d case), as we can see, they are worth implementing for modeling flows with complex vortex structures.

Nevertheless, for the future work it might be prudent to investigate behavior of the eddy viscosity models with anisotropic corrections for the flows of the considered type.

Conclusion. Based on the analysis of the obtained data and their comparison with the experiments, the following conclusions can be drawn.

When calculating the flow in the base region and in the wake of the vehicle, it is very important to take into account the "prehistory" of the flow, i.e., to calculate the flow around the entire vehicle.

To better describe the velocity distribution in the base region, it is recommended to use models of RS type, which confirms the superiority of the models of this type over simpler eddy-viscosity models such as *k*–ε and SST, the main shortcoming of which, is their inability to account for history of flow upstream which influences motions of the larger scale eddies and contributes to the transfer of scalar quantities such as turbulent energy (see [15, 16]).

REFERENCES

[1] Kawai S., Fujii K. Computational study of a supersonic base flow using hybrid turbulence methodology. *AIAA J.,* 2005, vol. 43, no. 6, pp. 1265–1275.
DOI: https://doi.org/10.2514/1.13690

[2] Guoliang L., Liu Q., Yang Y., et al. Study on supersonic base flow with and without plume interaction. *AIAA Paper*, 2017, no. 2017-2276.
DOI: https://doi.org/10.2514/6.2017-2276

[3] Nazarov F.Kh. Comparing turbulence models for swirling flows. *Herald of the Bauman Moscow State Technical University, Series Natural Sciences*, 2021, no. 2 (95), pp. 25–36 (in Russ.). DOI: https://doi.org/10.18698/1812-3368-2021-2-25-36

[4] Herrin J.L., Dutton J.C. Supersonic base flow experiments in the near wake of a cylindrical afterbody. *AIAA J.*, 1994, vol. 32, no. 1, pp. 77–83.
DOI: https://doi.org/10.2514/3.11953

[5] Molchanov A.M. Neravnovesnaya vysokoental'piynaya termogazodinamika [Non-equilibrium high-enthalpy thermogasdynamics]. Moscow, MAI Publ., 2020.

[6] Wilcox D.C. Turbulence modeling for CFD. DCW industries, 2006.

[7] Mathur T., Dutton J.C. Base-bleed experiments with a cylindrical afterbody in supersonic flow. *J. Spacecr. Rockets.*, 1996, vol. 33, no.1, pp. 30–37.
DOI: https://doi.org/10.2514/3.55703

[8] Catalano G.D., Sturek W.B. A numerical investigation of subsonic and supersonic flow around axisymmetric bodies. Storming Media, 2001.

[9] Molchanov A.M. Numerical simulation of supersonic chemically reacting turbulent jets. *AIAA Paper,* 2011, no. 2011-3211. DOI: https://doi.org/10.2514/6.2011-3211

[10] Molchanov A.M., Siluyanova M.V., Kochetkov Yu.M. The implicit fully coupled numerical method for flows in thermochemical nonequilibrium. *IOP Conf. Ser.: Mat. Sc. Eng.*, 2020, vol. 927, art. 012005.
DOI: https://doi.org/10.1088/1757-899X/927/1/012005

[11] Kochetkov Y.M., Molchanov A.M., Siluyanova M.V. Calculation of high-altitude jets of the rocket engine based on quasi-gasdynamic equations. *Russ. Aeronaut.*, 2019, vol. 62, no. 3, pp. 423–428. DOI: https://doi.org/10.3103/S1068799819030097

[12] Gidaspov V.Y., Kononov D.S., Severina N.S. Simulation of the ignition and detonation of methane–air mixtures behind a reflected shock wave. *High Temp.*, 2020, vol. 58, no. 6, pp. 846–851. DOI: https://doi.org/10.1134/S0018151X20060103

[13] Ryzhkov S.V., Kuzenov V.V. Analysis of the ideal gas flow over body of basic geometrical shape. *Int. J. Heat Mass Transf.*, 2019, vol. 132, pp. 587–592.
DOI: https://doi.org/10.1016/j.ijheatmasstransfer.2018.12.032

[14] Kuzenov V.V., Ryzhkov S.V. Approximate calculation of convective heat transfer near hypersonic aircraft surface. *J. Enhanc. Heat Transf.*, 2018, vol. 25, iss. 2, pp. 181–193. DOI: https://doi.org/10.1615/jenhheattransf.2018026947

[15] Nezu I., Nakagawa H. Turbulence in open-channel flows. CRC Press, 1993.

[16] Pope S.B. Simple models of turbulent flows. *Phys. Fluids*, 2011, vol. 23, iss. 1, art. 011301. DOI: https://doi.org/10.1063/1.3531744

Molchanov Aleksandr M. — Dr. Sc., Assoc. Professor, Department of Thermal Engineering, Moscow Aviation Institute (National Research University) (Volokolamskoe shosse 4, Moscow, 125993 Russian Federation).

Yanyshev Dmitry S. — Cand. Sc., Assoc. Professor, Department of Thermal Engineering, Moscow Aviation Institute (National Research University) (Volokolamskoe shosse 4, Moscow, 125993 Russian Federation).

Bykov Leonid V. — Cand. Sc., Assoc. Professor, Department of Thermal Engineering, Moscow Aviation Institute (National Research University) (Volokolamskoe shosse 4, Moscow, 125993 Russian Federation).

Please cite this article as:

Molchanov A.M., Yanyshev D.S., Bykov L.V. Numerical investigation of a supersonic flow in the near wake region of a cylindrical afterbody. *Herald of the Bauman Moscow State Technical University, Series Natural Sciences*, 2022, no. 3 (102), pp. 86–95. DOI: https://doi.org/10.18698/1812-3368-2022-3-86-95